A MODEL FOR ANALYSIS OF POROUS GAS ELECTRODES

E. A. Grens II,* R. M. Turner, and T. Katan

Materials Sciences Laboratory
Lockheed Missiles & Space Company
Sunnyvale, California

The porous gas electrode, usually with oxygen or hydrogen as the reactant gas, has found wide application in fuel cell systems. The charge transfer reactions for such electrodes occur under conditions quite different from those at a plane electrode surface; the transport of current and reacting species to and from the reaction sites and the location of these sites must be considered in establishing overpotential-current density curves for these half cells. Several investigators have considered this problem, and from several separate points of view (1 – 5). Various models have been used, corresponding to different liquid configurations in the pores, to different methods of reactant transport, and to different local electrode overpotential relationships at the reaction site. The results have varied as widely as the models. Some may correspond to one type of electrode, electrolyte, and operation; some to another. The present treatment analyzes porous gas electrodes in which the electrolyte wets the pore walls. This situation commonly occurs, except where pore walls have been purposefully rendered lyophobic to prevent flooding, a practice necessary only where the electrolyte gas interface is not fixed by pore geometry.

The ability of the electrolyte to wet the pore walls generates a liquid film covering the walls of part of the gas-filled portion of the pore. The electrode reaction takes place beneath some portion of this film, where the gaseous reactant can reach the reactant site. Will (4) has shown that the reactant must be supplied by diffusion of dissolved gas through the film. However, in Will's analysis of his model, assumptions are made which restrict consideration to those cases where dissolved gas diffusion is the only rate-determining process. This can be the case only where reaction exchange current densities are large compared with the limiting diffusion currents through the film. Since the latter must be on the order of 0.02 amp/cm^2 in pores of micron order,** exchange current densities larger than usually accepted for many gas reactions (e. g., O_2) would be necessary for diffusion control. The influence on electrode performance of dissolved gas diffusion, local overpotential, and transport of current and ionic products are all considered in the analysis presented in this paper.

ELECTRODE MODEL

A porous electrode consists of a very complex arrangement of interconnected voids or pores in a conducting solid matrix. For simplicity of description, however, an idealized pore structure consisting of parallel, straight tubes of circular cross section may be adopted. Each such pore is in part filled with electrolyte, the remainder being occupied by the gas phase.

---

*Department of Chemical Engineering, University of California, Berkeley

**For a diffusion coefficient, D_g, of 10^{-5} cm^2/sec, a gas solubility of 2×10^{-7} gmol/cm^3, and a film thickness of 0.1μ, the diffusion current is

$$\frac{D_g c_g^o}{\delta} F = \frac{(10^{-5})(2 \times 10^{-7})(10^5)}{10^{-5}} = 2 \times 10^{-2} \text{ amp/cm}^2$$

The diameter of such pores may be taken as slowly varying compared with the diameter itself. A changing diameter is necessary for a stable liquid meniscus at constant differential pressure. Thus, one of the many pores present in the electrode may be represented as in Fig. 1. The transport of reactant and product species, and of current, may be considered for three basic regions of the pore: first, transport of ionic species in the electrolyte in the pore up to the meniscus; second, phenomena in the reaction zone; and third, transport of gas reactant in the gas-filled part of the pore. The first of these effects may be important in many cases but is easily treated by standard electrolytic mass transport techniques (6); it should be kept small in well-designed electrodes. The third effect is absent for pure gas reactants and is readily treated otherwise (6). The treatment here is concerned with the reaction zone, the most critical area in electrode performance.

The meniscus and the associated electrolyte film which wets the pore wall for a very long distance into the gas region may be simplified to the representation shown in Fig. 2, so long as the reaction occurs over a length of film that is long compared with the meniscus dimensions. This will later be shown to be the case under most operating conditions. Here the meniscus is assumed to be flat, dropping directly to the constant film thickness, δ, which covers the wall for a distance equivalent to many times its thickness. The reaction is assumed to occur entirely at the pore wall beneath this film. This implies a negligible portion of reaction occurring at the walls of the liquid-filled portion of the pore, a condition verified by the data of Will (4). Moreover, it is shown in the Appendix that current which can be generated by reactions in this region are small compared with most current drains that would be encountered in operating fuel cell systems. The film thickness is taken as sufficiently small, compared with pore diameter, that the wall curvature may be disregarded and a unit width of film on an essentially plane surface investigated.

The electrode reaction for this model is the general gas reaction

$$G + ne^- \rightarrow \mu H_2O + \nu S_1^{Z_1} \tag{1}$$

where G represents the chemical symbol for some reactant gas and S_1 that for an ionic species of charge Z_1 which participates in the reaction; μ and ν are stoichiometric coefficients. For this reaction, a realistic overpotential expression of the redox or Erdey-Gruz type is used [see Vetter (7)], giving a transfer current density

$$j^s = j_o \left\{ \frac{c_g}{c_g^o} \exp\left[\frac{\alpha m F}{RT}(\phi - \phi_e)\right] - \frac{c_1}{c_1^o} \exp\left[\frac{(\alpha - 1)\, mF}{RT}(\phi - \phi_e)\right] \right\} \tag{2}$$

This expression is characterized by the exchange current density, j_o, and the equilibrium potential, ϕ_e, at bulk electrolyte concentration, c_1^o, and gas saturation, c_g^o. It should be noted that the electron transfer in the rate-determining step m is not necessarily the overall electron transfer n.

In treating the electrode model, the following assumptions are invoked:

1. Isopotential electrode matrix
2. Uniform gas phase composition
3. Constant transport parameters
4. Electrolyte saturated with reactant gas at gas liquid interface
5. Isothermal operation

The examination is restricted to cases in which only one significant nonreacting ionic species, S_2, is present.

The transport of chemical species and current in the film are governed by the fundamental flux equations for electrolytes. For a species i , the flux, $\underline{N}_i$, in the absence of hydrodynamic flow, is

$$\underline{N}_i = - D_i \nabla c_i - z_i u_i \epsilon \nabla \phi \tag{3}$$

The current density, i , in the film is then

$$\underline{i} = F \sum_{\text{SPECIES}} z_i \underline{N}_i \tag{4}$$

For electrolyte systems (at points outside the electric double layer) the electroneutrality condition may be used in place of the potential (Poisson) equation. This condition is

$$\sum_{\text{SPECIES}} z_i c_i = 0 \tag{5}$$

Using the assumptions enumerated above, along with the Nernst-Einstein relation, $u_i = D_i/kT$, which is of the same order of approximation as assumption (3), the steady-state transport equations for the model may be derived. For the ionic species, fluxes must be almost entirely in the x direction because of the thinness of the film.

$$N_1 = - D_1 \frac{dc_1}{dx} - D_1 \frac{Fz_1}{RT} c_1 \frac{d\phi}{dx} \tag{6}$$

$$N_2 = - D_2 \frac{dc_2}{dx} - D_2 \frac{Fz_2}{RT} c_2 \frac{d\phi}{dx} = 0 \tag{7}$$

The flux of the nonreacting species is, of course, zero at steady state, as shown. The dissolved gas diffuses through the film, having a significant flux only in the y direction.

$$N_g = - D_g \frac{dc_g}{dy} \tag{8}$$

The current in the film is carried only by species 1 and is thus

$$i = z_1 F N_1 \tag{9}$$

These equations have the following boundary conditions:

$$\begin{aligned} &\text{at } x = 0\text{: } c_1 = c_1^o \text{ ; } c_2 = c_2^o \text{ ; } \phi = \phi^o \\ &x = \infty\text{: } \frac{dc_1}{dx} = \frac{dc_2}{dx} = \frac{d\phi}{dx} = 0 \\ &y = \delta\text{: } c_g = c_g^o \end{aligned} \tag{10}$$

Since a change in current per unit width of film, $i\delta$, can occur only by a transfer to the pore wall, i can be related to j^s of Eq. (2) by

$$\frac{di}{dx} = -\frac{j^s}{\delta} \tag{11}$$

Similarly, the flux of dissolved gas must correspond to the reaction rate at the pore wall at the same value of x, giving

$$N_g = -\frac{j^s}{nF} = \frac{\delta}{nF}\frac{di}{dx} \tag{12}$$

If now the electroneutrality condition (5) is substituted into Eq. (7); Eq. (6) is inserted into Eq. (9); Eq. (12) is combined with Eq. (8); and the transformation to dimensionless form,

$$C = \frac{c_1}{c_1^o} \quad ; \quad Y = \frac{y}{\delta}$$

$$G^* = \frac{c_g}{c_g^o} \quad ; \quad X = \frac{x}{\delta} \tag{13}$$

$$\Phi = \frac{F}{RT}(\phi - \phi_e) \quad ; \quad I = \frac{-i\delta}{z_1 F D_1 c_1^o}$$

is introduced, the equation system describing the film model becomes

$$\frac{dC}{dX} = -z_2 C \frac{d\Phi}{dX} \tag{14}$$

$$I = \frac{dC}{dX} + z_1 C \frac{d\Phi}{dX} \tag{15}$$

$$\frac{dG^*}{dY} = -\Omega \frac{dI}{dX} \tag{16}$$

and the overpotential expression (2) takes on the form

$$\frac{dI}{dX} = -\gamma \left\{ G \exp\left[\alpha m \Phi\right] - C \exp\left[(\alpha - 1)\, m\Phi\right] \right\} \tag{17}$$

where G is the value of G^* at $Y = 0$ and the dimensionless parameters Ω and γ are

$$\Omega = \frac{-z_1 D_1 c_1^o}{n D_g c_g^o}$$

$$\gamma = \frac{-j_o \delta}{z_1 F D_1 c_1^o} \tag{18}$$

The boundary conditions (10) are:

$$\text{at } X = 0: \; C = 1, \; \Phi = \Phi^o = \frac{F}{RT}\left(\phi^o - \phi_e\right)$$

$$X = \infty: \; \frac{dC}{dX} = \frac{d\Phi}{dX} = 0 \tag{19}$$

$$Y = 1: \; G^* = 1$$

Integrating Eq. (14) and substituting in Eq. (15) gives

$$\frac{d\Phi}{dX} = \frac{I}{z_1 - z_2} e^{z_2(\Phi - \Phi^o)} \tag{20}$$

Also integrating Eq. (16) and substituting this and the previous integrated result for C in Eq. (17) yields

$$\frac{dI}{dX} = \frac{1}{\Omega + \frac{1}{\gamma} e^{-\alpha m \Phi}} \left\{ e^{z_2 \Phi^o} e^{-(z_2 + m)\Phi} - 1 \right\} \tag{21}$$

Equations (20) and (21), taken together with the conditions

$$\text{at } X = 0: \; \Phi = \Phi^o \; ; \; \text{at } X \to \infty \; ; \; I = \frac{dI}{dX} = 0 \tag{22}$$

are amenable to analog computer solution. Such a solution, applied to the oxygen electrode in 5M KOH, is discussed in a following section.

APPROXIMATE ANALYSIS FOR LOW ELECTRODE OVERPOTENTIALS

To obtain analytic solutions for the model, it is necessary to restrict consideration to cases where the overpotential is small. Then perturbation of a basic condition in which no current flows can describe behavior of the model.

The variables of the system may be broken down into those representing the nonperturbed condition, G_o, C_o, Φ_o, I_o, and small perturbations G', C', Φ', I'. For the unperturbed state characterized by no current flow,

$$G_o = 1 \; ; \; C_o = 1 \; ; \; \Phi_o = \Phi^o \; ; \; I_o = 0 \tag{23}$$

and the variables with perturbations are

$$\begin{aligned} G &= G_o + G' = 1 + G' \\ C &= C_o + C' = 1 + C' \\ \Phi &= \Phi_o + \Phi' = \Phi^o + \Phi' \\ I &= I' \end{aligned} \tag{24}$$

Then Eqs. (14) and (15) and the integrated form of Eq. (16) become

$$\frac{dC'}{dX} = - z_2 (1 + C') \frac{d\Phi'}{dX} \tag{25}$$

$$I' = \frac{dC'}{dX} + z_1 (1 + C') \frac{d\Phi}{dX} \tag{26}$$

$$G' = \Omega \frac{dI'}{dX} \tag{27}$$

and the overpotential relation (17) appears as

$$\frac{dI'}{dX} = - \gamma \left\{(1 + G') \exp \left[\alpha m (\Phi^o + \Phi')\right] - (1 + C') \exp \left[(\alpha - 1) m(\Phi^o + \Phi')\right]\right\} \tag{28}$$

Neglecting second-order terms and expanding the exponentials in Eq. (28), these equations take the linear forms

$$\frac{dC'}{dX} = - z_2 \frac{d\Phi'}{dX} \tag{29}$$

$$I' = \frac{dC'}{dX} + z_1 \frac{d\Phi'}{dX} \tag{30}$$

$$\frac{dI'}{dX} = - \gamma e^{\alpha m \Phi^o} \left\{1 + G' + \alpha m \Phi' - \left[1 + C' + (\alpha - 1) m\Phi'\right] e^{-m\Phi^o}\right\} \tag{31}$$

Combining Eqs. (29) and (30) yields

$$\frac{dC'}{dX} = \frac{z_2}{z_2 - z_1} I' \quad ; \quad \frac{d\Phi'}{dX} = \frac{- 1}{z_2 - z_1} I' \tag{32}$$

Then differentiating Eq. (31) with respect to X and substituting for $\frac{dC'}{dX}$, $\frac{d\Phi'}{dX}$, and $\frac{dG'}{dX}$ from Eqs. (32) and (27) gives

$$\frac{d^2I'}{dX^2} = - \gamma e^{\alpha m \Phi^o} \left\{\Omega \frac{d^2I'}{dX^2} - \left(\alpha m + \left[z_2 - (\alpha - 1) m\right] e^{-m\Phi^o}\right)\left(\frac{I'}{z_2 - z_1}\right)\right\} \tag{33}$$

But, since I' is I, this rearranges to just

$$\frac{d^2I}{dX^2} = \frac{I}{L^2} \tag{34}$$

where

$$L^2 = \frac{\Omega + \frac{1}{\gamma} e^{-\alpha m \Phi^o}}{\alpha m + (z_2 + m - \alpha m) e^{-m\Phi^o}}$$

Equation (34) is easily solved with the condition of Eq. (19) at $X \to \infty$ to yield the expression

$$I = I^o e^{-\frac{X}{L}} \tag{35}$$

The equivalent expressions for C and Φ are easily determined from Eqs. (32) and (24).

$$C = 1 + \frac{z_2}{z_2 - z_1} LI^o \left(1 - e^{-\frac{X}{L}}\right) \tag{36}$$

$$\Phi = \Phi^o + \frac{1}{z_2 - z_1} LI^o \left(e^{-\frac{X}{L}} - 1\right) \tag{37}$$

In all these solutions, the constant I^o, representing current in the film at the meniscus ($X = 0$), appears. This quantity is determined by substituting dI/dX obtained from Eq. (35) into Eq. (17) evaluated at $X = 0$. This gives the result

$$I^o = L \frac{1 - e^{-m\Phi^o}}{\Omega + \frac{1}{\gamma} e^{-\alpha m\Phi^o}} = \frac{1 - e^{-m\Phi^o}}{\sqrt{\left(\Omega + \frac{1}{\gamma} e^{-\alpha m\Phi^o}\right)\left(\alpha m + (z_2 + m - \alpha m) e^{-m\Phi^o}\right)}} \tag{38}$$

These approximate solutions are valid only for small values of Φ^o. By comparison with analog computer solutions developed in the next section, it appears that they can be used for values of $\Phi^o \leq 0.5$ with good accuracy. (See Fig. 5.) This includes single electrode overpotentials (at 25°C) less than 12 mv, a considerable restriction. However, at $\Phi^o = 1$ the approximate solutions deviate by only about 25 percent; thus, they may be used over a wider range of operation for qualitative predictions.

The quantity L is characteristic of the length of the film over which reaction takes place. Its magnitude in commonly encountered situations (e.g., $10^3 - 10^4$ for the O_2 electrode in 5 M KOH) indicates that the original conditions assumed in simplifying meniscus shape are well justified.

ANALOG COMPUTER SOLUTIONS

Equations (20) and (21) have been analyzed on an Electronic Associates Type 131-R analog computer, mechanized as shown in Fig. 3. The solution is carried out by assuming I^o and checking the approach of I and (dI/dX) to 0 as X becomes very large. Behavior at large X is used to correct I^o for given Φ^o until all boundary conditions are satisfied.

The analog solution has been carried out for the case of the oxygen electrode in 5 M KOH. For this system, the following values were utilized (at 25°C):

$$z_1 = -1 \quad ; \quad z_2 = +1$$

$$c_1^o = 5 \times 10^{-3} \text{ gmol/cm}^3 \quad ; \quad c_g^o = 2 \times 10^{-7} \text{ gmol/cm}^3$$

$$D_1 = 4 \times 10^{-5} \text{ cm}^2/\text{sec} \quad ; \quad D_g = 1 \times 10^{-5} \text{ cm}^2/\text{sec}$$

$$n = 4 \quad ; \quad m = 3 \quad ; \quad \alpha = 0.5$$

The exchange current density was assumed at 10^{-4} amp/cm^2 (there being no well established values for this reaction), and values of film thickness of 10^{-4}, 10^{-5}, and 10^{-6} cm were investigated. This gave values of the parameters of the model as

$$\Omega = 2.5 \times 10^{4}$$

$$\gamma = 5 \times 10^{-7} \quad , \quad 5 \times 10^{-8} \quad , \quad \text{and} \quad 5 \times 10^{-9}$$

The analog computer produced curves of I and $-(dI/dx)$ (reaction rate) versus X as shown in Fig. 4 for one case studied ($\Phi^o = 1.0$, $\gamma = 5 \times 10^{-8}$). Comparison of solutions over a range of values of overpotential, Φ^o, results in curves of inlet film current, I^o, and characteristic active length, L, versus electrode overpotential, Φ^o, as shown in Figs. 5 and 6. It must be remembered that the graphs are of the dimensionless variables, conversion to single electrode overpotential, $\phi^o - \phi_e$, in volts, and superficial current density, j, in amp/cm^2, being according to

$$\phi^o - \phi_e = \frac{RT}{F} \Phi^o \qquad \text{volts} \tag{39}$$

$$j = - \frac{2pz_1 FD_1 c_1^o}{r} I^o \ \text{amp/cm}^2 \tag{40}$$

or for this example with a 50 percent porosity and 1μ pore, $\phi^o - \phi_e \simeq 0.025\ \Phi^o$ volts; $j = 400\ I^o$ amp/cm^2.

The results of the approximate solution for this example are plotted in Figs. 5 and 6. The close agreement for values of Φ^o less than 0.5 is apparent.

CONCLUSIONS

This investigation of porous gas electrodes with wetting electrolytes has established two significant points about the behavior of such systems. First, except for reactions of very high exchange current densities at the conditions in the pores ($> 10^{-2}$ amp/cm^2 referred to elemental surface area), the diffusion of reactant gas through the film on the pore wall is not a controlling effect for the majority of the area over which reaction occurs. Second, significant reaction rates exist at the wall under the electrolyte film at distances from the "intrinsic" meniscus equal to thousands of film thicknesses.

The extent of dissolved gas diffusion control can be seen by examination of Eq. (21). The effect of this diffusion manifests itself only when the term Ω is large compared with the term $\exp(-\alpha m\Phi/\gamma)$ (both terms in the denominator on the right-hand side). This condition can exist, for values of Ω and γ possible for gas electrodes, only if Φ is quite large (say ≥ 5) – that is, only if the electrode overpotential, Φ^o, is large. Even then, gas diffusion controls only at positions near the meniscus. For diffusion control throughout the entire reaction zone, Φ^o must exceed perhaps 20 or 25. This corresponds to few cases of electrode operation.

The prediction of significant reaction rates under the film at distances of $10^3 - 10^4$ film thickness from the meniscus involves a considerably longer reaction zone than the ~ 200 film thicknesses proposed by Will (4) for a similar model (for H_2 in acid). This difference is due principally to Will's assumption of no local overpotential except that due to dissolved gas concentration. This condition would give considerably higher local reaction rates, and thus a narrower reaction zone. It is equivalent to setting γ to ∞ in Eq. (21) (with perhaps some adjustment in the coefficients of Φ) and corresponds to the physical case of infinite exchange current density. The assumption is not realistic for most electrode reactions.

In addition to the general conclusions mentioned above, this analysis has yielded approximate expressions for overpotential-current density behavior and for current distribution in gas electrodes at low to moderate overpotentials, and a method of analog computation to determine these relationships under any reasonable conditions.

NOTATION

English Letters

c_i	concentration of species i in electrolyte (gmol/cm^3)
c_i^o	reference concentration of species i (gmol/cm^3)
D_i	diffusion coefficient of species i (cm^2/sec)
F	Faraday's constant (96,500 coul/equiv.)
i	current density in electrolyte film (amp/cm^2)
j	superficial current density for electrode (amp/cm^2)
j_o	exchange current density of electrode reaction (amp/cm^2)
j^s	local transfer current density due to reaction (amp/cm^2)
k	Boltzmann constant
m	number of electrons transferred in rate-determining reaction step
N_i	flux of species i in electrolyte (gmol/cm^2-sec)
n	number of electrons transferred in overall electrode reaction
p	electrode porosity
R	gas constant
r	pore radius (cm)
S_i	chemical symbol of species i
T	absolute temperature (°K)
u_i	mobility of species i (cm/sec-dyne)
x	distance coordinate along film (cm)
y	distance coordinate across film (cm)
z_i	charge number of species i

Greek Letters

α	transfer coefficient
δ	film thickness (cm)
ϵ	electronic charge
μ, ν	stoichiometric coefficients
ϕ	potential in electrolyte film (volts)
ϕ_e	equilibrium electrode potential at c_i^o (volts)

Subscripts

g	refers to dissolved reactant gas
1	refers to ionic species involved in electrode reaction
2	refers to nonreacting ionic species

ACKNOWLEDGMENT

The authors wish to acknowledge the financial support of this research by the U. S. Navy, Bureau of Weapons, under research contract NOw 60-0738-d.

LITERATURE CITED

1. Justi, E., Pilkuhn, M., Scheibe, W., and Winsel, A., "High-Drain Hydrogen Electrodes Operating at Ambient Temperature and Low Pressure," Verlag d. Akademie d. Wissenschaften u. d. Literatur, 1959.

2. Urbach, H. B., "Theory of Polarization of Gaseous-Diffusion Electrodes," in Fuel Cells, G. J. Young, ed., Reinhold, New York, 1963, p. 77.

3. Austin, L. G., "Polarization at Diffusion Electrodes," in Fuel Cells, op. cit., p. 95.

4. Will, F. G., J. Electrochem. Soc., 110, 152 (1963).

5. Meissner, H. P., and Reti, A. R., "Predicted Performance of an Air Electrode," paper presented at 50th National A. I. Ch. E. meeting, Buffalo, N.Y., 1963.

6. Winsel, A. W., "Improved Calculation of Polarization of Porous Electrodes," paper presented at Symposium on Porous Electrodes of The Electrochemical Society, Boston, 1962; also in Advanced Energy Conversion (in press).

7. Vetter, K. J., Elektrochemische Kinetik, Springer Verlag, Berlin, 1961, Sec. 49.

Appendix

ESTIMATE OF CONTRIBUTION OF ELECTRODE REACTION IN FLOODED PORTIONS OF THE PORES

To establish an estimate of the maximum contribution to electrode current arising in electrode reaction at the walls of the flooded portions of a pore (see Fig. 1), consider a one-dimensional analysis under conditions most favorable to such a reaction. If the coordinate system of Fig. 2 is utilized, the potential locus of such reaction is $-\infty < x < 0$. In this region, reactant gas supply is by diffusion essentially in the x direction.

$$N_g = - D_g \frac{dc_g}{dx} \tag{A. 1}$$

For conservation of dissolved gas at steady state,

$$0 = - \nabla \cdot N_g + \text{source term} = D_g \frac{d^2 c_g}{dx^2} - \frac{j^s a}{nF} \tag{A. 2}$$

where a is specific area of electrode based on pore volume (= 2/r for cylindrical pores). The overpotential expression (A. 2) may be simplified, for high electrolyte conductivity and constant ionic concentrations, to the approximation

$$j^s = A c_g - B \tag{A. 3}$$

where

$$A \simeq j_o \exp\left[\frac{\alpha m F}{RT}\left(\phi^o - \phi_e\right)\right] \quad ; \quad B \simeq j_o \exp\left[\frac{(\alpha - 1)\, mF}{RT}\left(\phi^o - \phi_e\right)\right]$$

This corresponds to pure gas diffusion control, which is to be expected for any reaction in this region. Substitution of Eq. (A.3) into Eq. (A.2) gives

$$\frac{d^2 c_g}{dx^2} = \frac{Aa}{nFc_g^o} c_g - B \tag{A.4}$$

which has the following boundary conditions:

$$\begin{aligned} &\text{at } x = 0 \quad : \; c_g = c_g^o \\ &x \to -\infty : \; \frac{dc_g}{dx} = c_g = 0 \end{aligned} \tag{A.5}$$

This equation has the solution, for the concentration gradient,

$$\frac{dc_g}{dx} = + \sqrt{\frac{Aa}{nFc_g^o} c_g^2 - \frac{Ba}{nF} c_g} \tag{A.6}$$

which corresponds to a flux of dissolved gas at the meniscus of

$$N_{g_{x=0}} = \left(- D_g \sqrt{\frac{a}{nF} c_g} \sqrt{\frac{A}{c_g^o} c_g - B} \right)_{x=0} = - D_g \sqrt{\frac{a}{nF} c_g^o} \cdot \sqrt{j^s_{x=0}} \tag{A.7}$$

or to a total superficial current density resulting from reaction in the flooded portion of the pores, j^f, of

$$j^f = - nFN_g = D_g \sqrt{anFc_g^o \, j^s_{x=0}} \tag{A.8}$$

Since $j^s_{x=0}$ cannot be much greater than j_o for the reaction, this contribution is very small indeed. For the oxygen electrode treated in the text, with $a = 10^5$ cm^2/cm^3,

$$j^f \leq (10^{-5}) \left[(10^5)(4)(10^5)(2 \times 10^{-7})(10^{-4}) \right]^{1/2} \simeq 10^{-5} \text{ amp/cm}^2$$

which is negligible. Even if the exchange current density were as high as 1 amp/cm^2, this contribution to superficial current density would be less than 10^{-3} amp/cm^2.

Thus, reaction in the flooded portion of the pores can be ignored if a film is present.

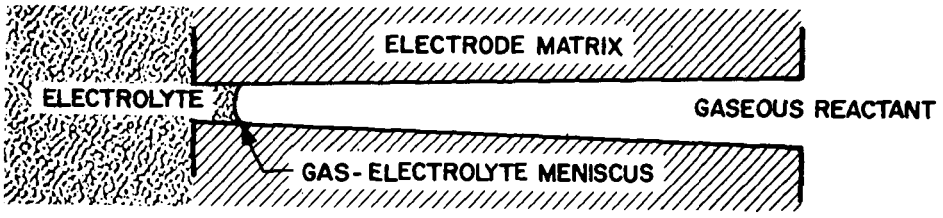

Fig. 1 Idealized Pore of Gas Electrode

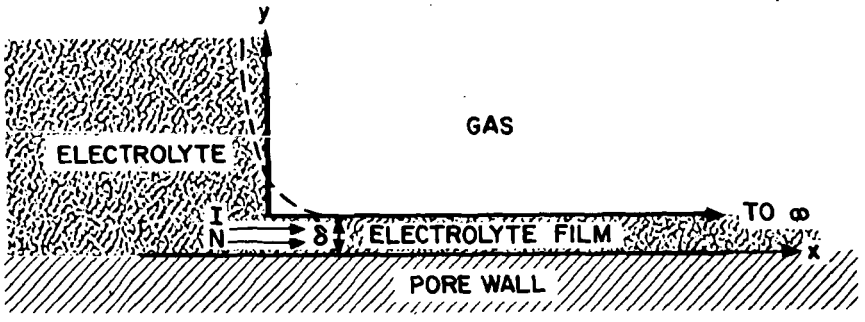

Fig. 2 Model for Reaction Zone of Porous Gas Electrode

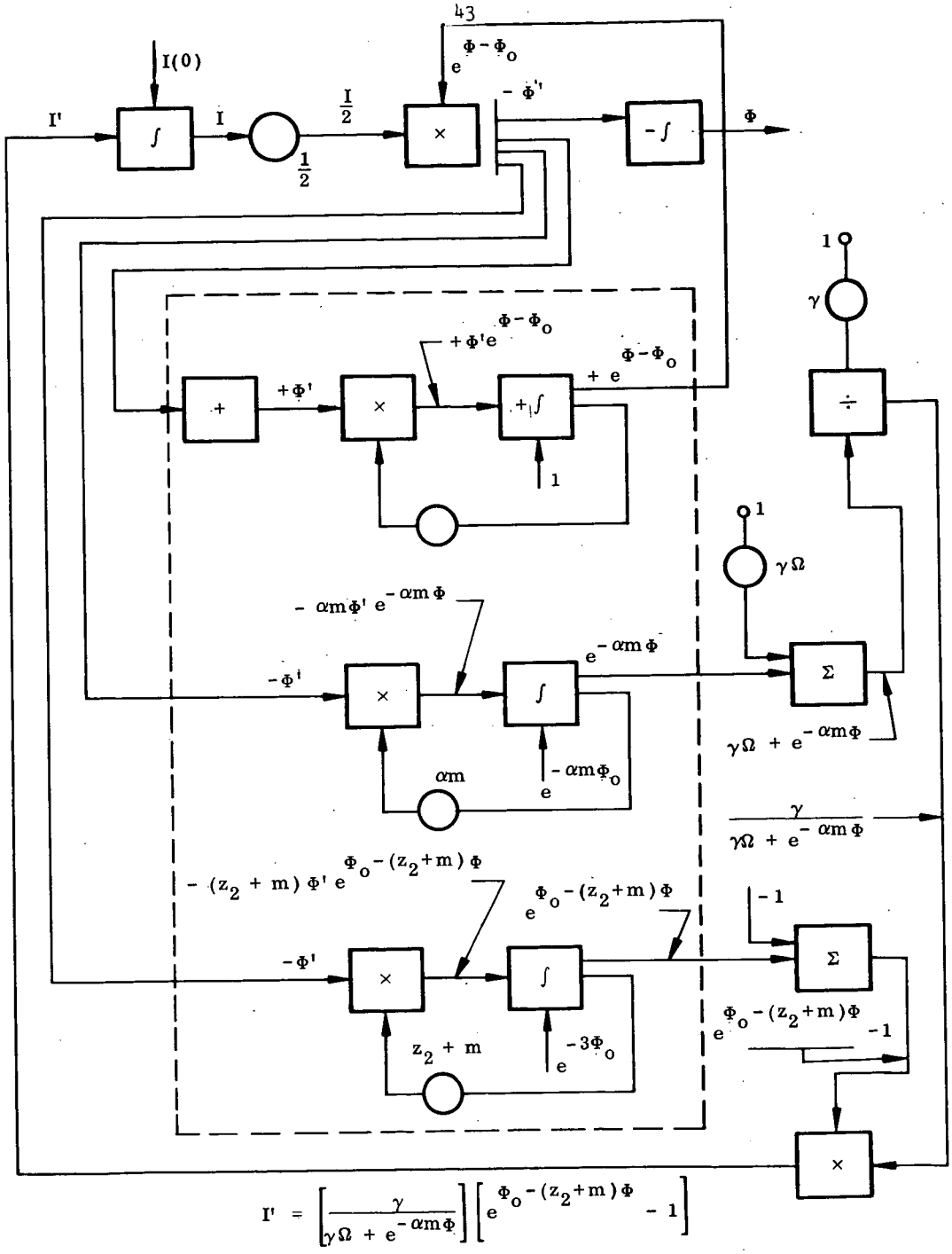

$$I' = \left[\frac{\gamma}{\gamma\Omega + e^{-\alpha m \Phi}}\right]\left[e^{\Phi_o - (z_2+m)\Phi} - 1\right]$$

Fig. 3 Block Diagram of Analog Computer Mechanization

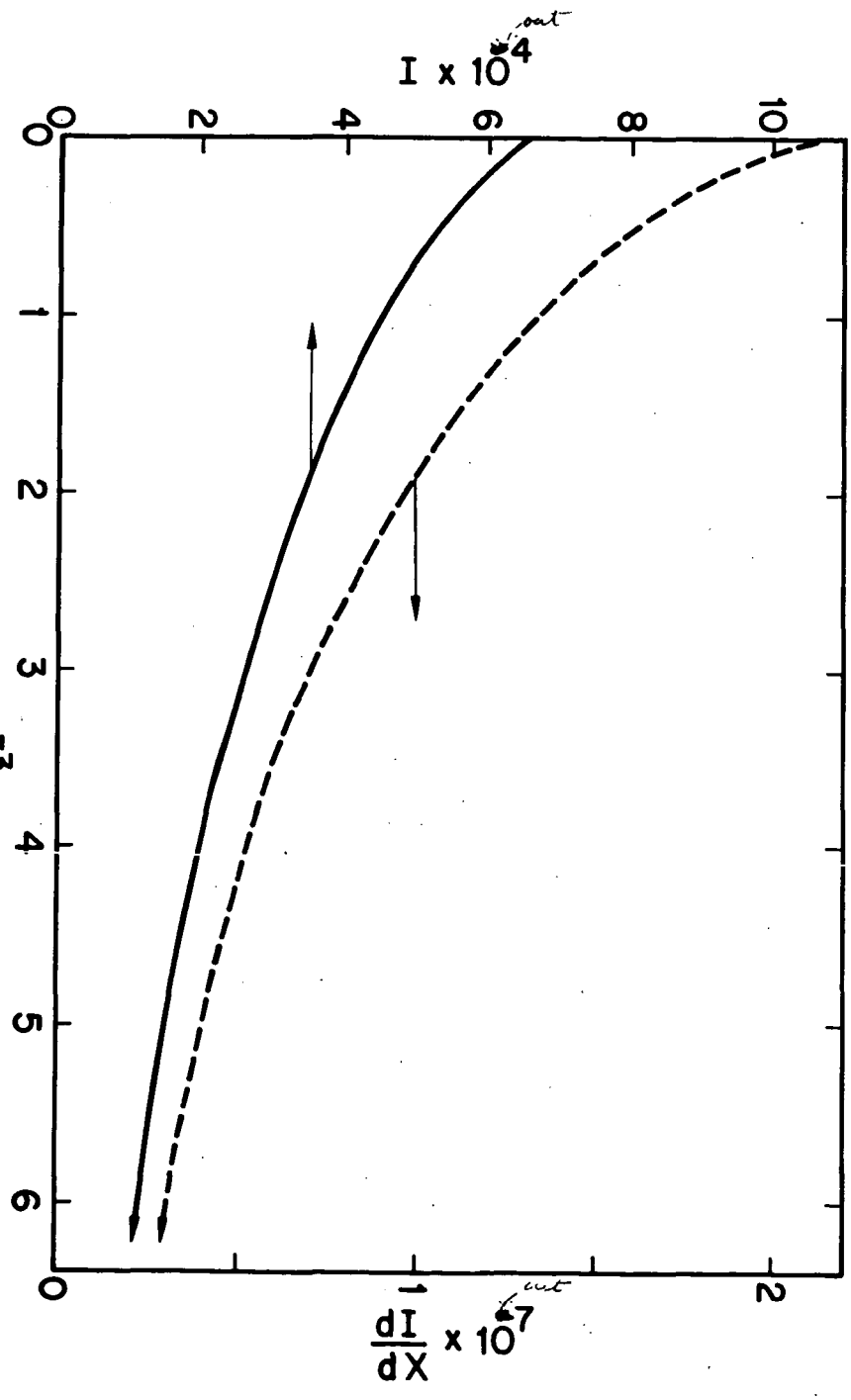

Fig. 4 Analog Computer Output Curves (Partial) for I and dI/dX Versus X for O_2 Electrode (KOH) ($\Omega = 2.5 \times 10^4$, $\gamma = 5 \times 10^{-8}$, $\Phi^\circ = 1.0$)

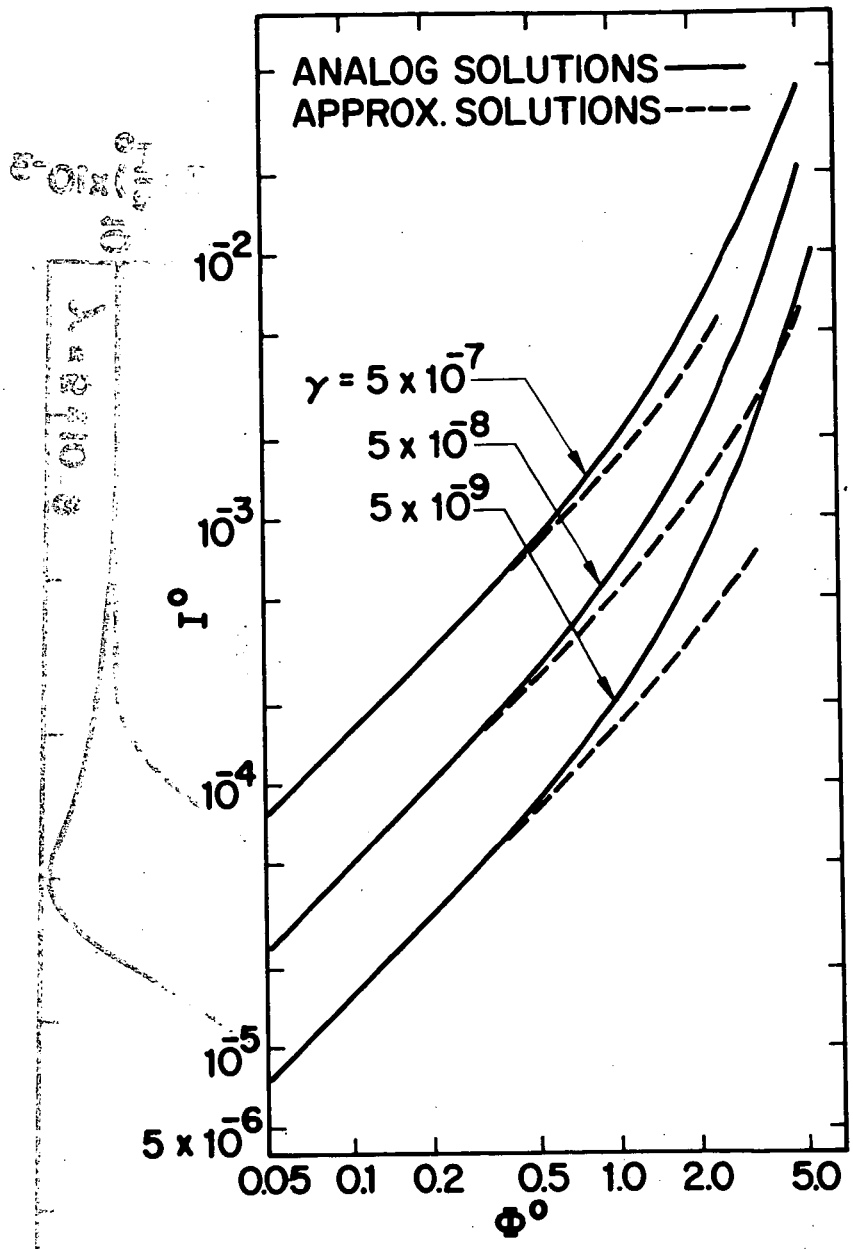

Fig. 5 Current–Overpotential Relations in Dimensionless Form for O_2 Electrode (KOH) ($\Omega = 2.5 \times 10^4$, γ as Shown)

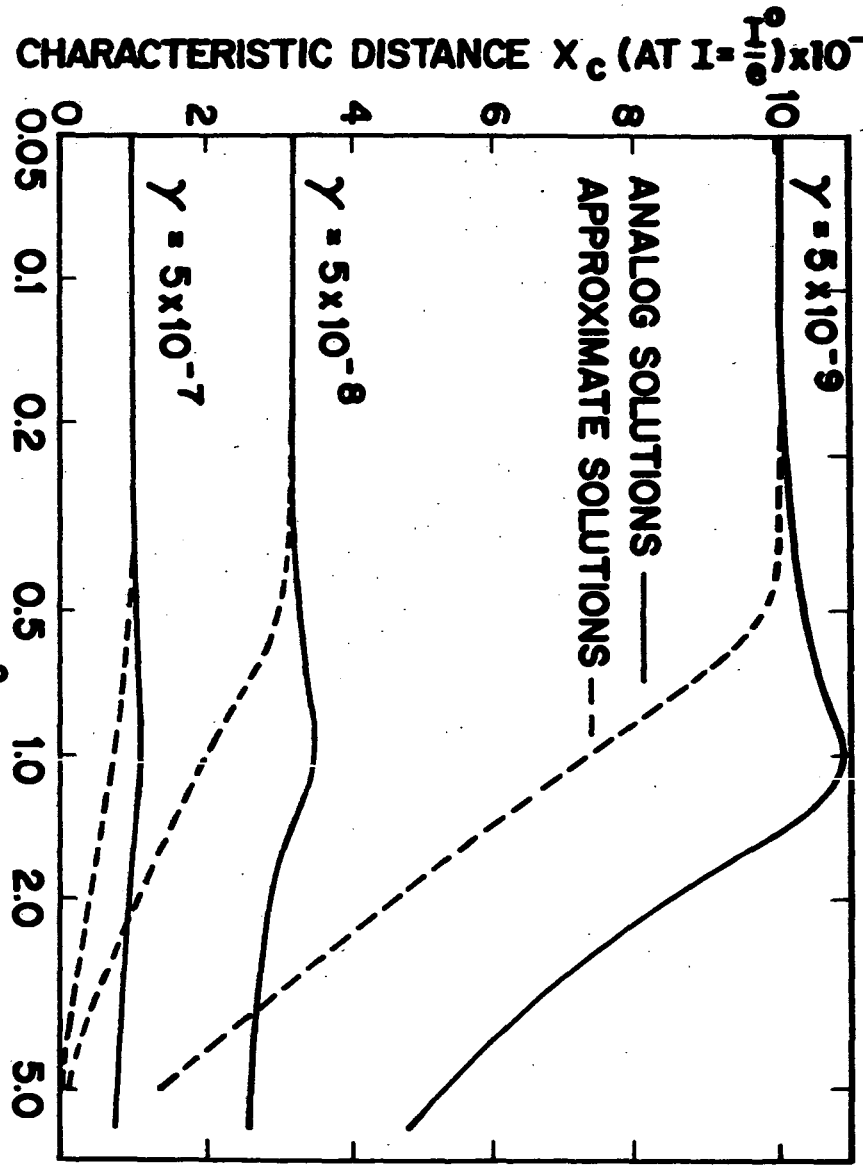

Fig. 6 Characteristic Distances for Active Length of Film Versus Overpotential for O_2 Electrode (KOH) ($\Omega = 2.5\times10^4$, γ as Shown)